THE JOURNAL OF BIOLOGICAL CHEMISTRY VOL. 288, NO. 15, pp. 10451–10458, April 12, 2013

Light-dark Adaptation of Channelrhodopsin C128T Mutant*[S]

Received for publication, December 18, 2012, and in revised form, February 15, 2013 Published, JBC Papers in Press, February 25, 2013, DOI 10.1074/jbc.M112.446427

Eglof Ritter[‡1], **Patrick Piwowarski**[‡], **Peter Hegemann**[§], **and Franz J. Bartl**[‡2]

From the [‡]*Institut für Medizinische Physik und Biophysik, Charité-Universitätsmedizin Berlin, Charitéplatz 1, 10117 Berlin, Germany and* [§]*Institut für Biologie, Humboldt-Universität zu Berlin, Unter den Linden 6, 10099 Berlin, Germany*

Background: Channelrhodopsins are light-gated ion channels of microalgae.
Results: By FTIR spectroscopy, we identified three different dark and two photoswitchable light-adapted states of the ChR-C128T mutant.
Conclusion: We propose a photocycle model that explains both spectroscopic and electrophysiological data.
Significance: Color-dependent equilibria determine the stationary photocurrents in ChR applications (optogenetics).

Channelrhodopsins are microbial type rhodopsins that operate as light-gated ion channels. Largely prolonged lifetimes of the conducting state of channelrhodopsin-2 may be achieved by mutations of crucial single amino acids, *i.e.* cysteine 128. Such mutants are of great scientific interest in the field of neurophysiology because they allow neurons to be switched on and off on demand (step function rhodopsins). Due to their slow photocycle, structural alterations of these proteins can be studied by vibrational spectroscopy in more detail than possible with wild type. Here, we present spectroscopic evidence that the photocycle of the C128T mutant involves three different dark-adapted states that are populated according to the wavelength and duration of the preceding illumination. Our results suggest an important role of multiphoton reactions and the previously described side reaction for dark state regeneration. Structural changes that cause formation and depletion of the assumed ion conducting state P520 are only small and follow larger changes that occur early and late in the photocycle, respectively. They require only minor structural rearrangements of amino acids near the retinal binding pocket and are triggered by all-*trans*/13-*cis* retinal isomerization, although additional isomerizations are also involved in the photocycle. We will discuss an extended photocycle model of this mutant on the basis of spectroscopic and electrophysiological data.

Channelrhodopsin (ChR)[3] is a microbial type rhodopsin that serves as a light-gated ion channel in the eye spot of green algae. As typical for rhodopsins, it exhibits seven transmembrane helices. Similar to bacteriorhodopsin and other microbial rhodopsins, it undergoes a photocycle initiated by light-induced isomerization of the retinal chromophore. Details of the molecular architecture of its dark-adapted state are now available owing to the crystal structure of a chimera between ChR1 and ChR2 (1). This structure allows the identification of residues in the retinal binding pocket and the putative cation-conducting pathway.

However, molecular changes that are linked to formation of the conducting pore and stabilization of the channel are not yet understood. Electrical measurements yielded the first information about the channelrhodopsin photocycle. On and off kinetics of the photocurrents has provided insights into the formation and decay of the conducting state in the microsecond time range (2, 3).

UV-visible absorption measurements on recombinant ChR identified two early photocycle intermediates, P500 and P380, that precede the conducting state P520 (2, 3). The latter decays within 10 ms, but complete regeneration of the dark state is slow and occurs in the time range of 20 s (4, 5). The late photocycle intermediate P480 is photochemically active; the photocurrents decline to a reduced stationary level upon repetitive or prolonged ChR2 stimulation. One solution for the interpretation of this observation comes from the ChR2 mutants called step function rhodopsin. In these mutants, Cys-128 is exchanged by threonine, serine, or alanine, thereby dramatically slowing down the lifetime of the conducting state. Additionally, these mutants can be switched on and off by blue and green light, respectively. These properties offer the opportunity to achieve a more permanent cell depolarization, where the lifetime of the open state can be controlled by flash or continuous low light intensities (6).

The photocycle of such mutants is however more complex than originally anticipated for the ChR2 wild type. It exhibits branches and side reactions that render step function rhodopsins nonfunctional after extended illumination (7–9). We previously suggested that the probability of photochemical side reactions increases with the lifetime of the corresponding state (8, 10). Despite these complications the slow kinetics of step function rhodopsins offers the opportunity to study the photocycle of Cys-128 in depth because they facilitate the application of FTIR spectroscopy, which allows the observation of the reaction mechanisms of channelrhodopsins at the molecular level.

In this study, we reinvestigated the photocycle of the slow cycling mutant C128T by a combination of FTIR and UV-visi-

* This work was supported by the Deutsche Forschungsgemeinschaft Grants BA 2242/2-1 (to F. J. B.) and SFB 1078.
[S] This article contains supplemental Figs. 1 and 2.
[1] To whom the correspondence may be addressed: Institut für Medizinische Physik und Biophysik, Charité, Universitätsmedizin Berlin, Charitéplatz 1, 10117 Berlin, Germany. Tel.: 49-30-450524196; Fax: 49-30-450-524-952; E-mail: eglof.ritter@charite.de.
[2] To whom the correspondence may be addressed: Institut für Medizinische Physik und Biophysik, Charité, Universitätsmedizin Berlin, Charitéplatz 1, 10117 Berlin, Germany. Tel.: 49-30-450524196; Fax: 49-30-450-524-952; E-mail: franz.bartl@charite.de.
[3] The abbreviations used are: ChR, channelrhodopsin; IDA, initial dark state; DAB, dark-adapted state after blue; DAG, dark-adapted state after green illumination.

ble spectroscopy and by retinal extraction with subsequent HPLC analysis. We show the existence of two dark intermediates that are populated depending on the wavelength and duration of the preceding illumination. Formation of the presumed ion conducting state P520 (channel gating) involves two distinct mechanistic steps. Formation and decay of a pre-conducting state occurs early and late in the photocycle and requires major backbone alterations. Second, a fast switch between a pre-conducting state and P520, triggered by all-*trans*/13-*cis* and/or *syn*/*anti* Schiff base isomerization requires only minor structural changes in or near the binding pocket. Finally, we present a model of the photocycle that links and explains both spectroscopic and electrophysiological findings.

EXPERIMENTAL PROCEDURES

Expression and Purification of Channelrhodopsin—Expression in COS cells and purification of channelrhodopsin mutants was performed as described previously (8) using a synthetic DNA fragment with a C-terminal ETSQVAPA sequence (1D4 epitope (11), GeneArt Regensburg). Mutations were generated by site-directed mutagenesis (QuikChange kit; Stratagene). Further preparation steps of the mutants (cell culture, transfection with the resulting ChR2-pMT4 vector, reconstitution with 30 μM all-*trans* retinal and subsequent purification of ChR2) was performed basically as described for bovine rhodopsin (12). L-α-Phosphatidylcholine (Avanti Polar Lipids, Inc., Alabaster, AL) lipid vesicles with a lipid:protein ratio of 100:1 were prepared by detergent dialysis as described (13) and concentrated with Centricon YM-10 concentrators. All preparation steps were performed under dim red light ($\lambda_{max} > 680$ nm). The samples were stored at −80 °C.

Illumination Protocol—All illuminations were performed with light-emitting diodes. Three blue (470 nm, 7200 mcd), green (520 nm, 10000 mcd) or UV (400 nm, 15000 mcd) light-emitting diodes (Winger Electronics GmbH and Co. KG, Dessau-Rosslau, Germany) were individually focused on the sample in the cuvette. Flash illuminations were achieved by switching on the light for 20 ms. For continuous illumination experiments, the reactions were followed spectroscopically, and the illumination was performed until a stationary state was reached. For HPLC analysis of the retinoids, the sample was illuminated correspondingly in a 2-ml Eppendorf tube.

Chromophore Isomer Analysis—10 μl of a 80 μM ChR2 stock solution was used for retinal isomer analysis. After illumination and appropriate incubation time, denaturation of the protein was achieved by addition of 100 μl of ice-cold ethanol. After 2 min of stirring on ice, retinals were extracted by addition of 100 μl of ice-cold heptane/ethyl acetate mixture (volume ratio 95:5) (14). After centrifugation, the upper heptane phase was then removed and concentrated by gently drying with nitrogen. Separation of the retinal isomers was performed in a heptane/ethyl acetate mixture (90/10 (v/v)) using a LC 20AD HPLC device (Shimadzu, Kyoto) equipped with a Li Chrosorb 60.5-μm column (CHROM, Herrenberg-Kayh).

FTIR and UV-visible Spectroscopy—FTIR sample preparation of ChR2 in L-α-phosphatidylcholine vesicles was done by a centrifugation procedure as described (15). The pellets containing ~2 mM ChR2 were measured in a temperature-controlled BaF_2 transmission cuvette with 3-μm optical pathlength. FTIR spectra were recorded with an IFS 66v/S spectrometer (Bruker Optik GmbH, Ettlingen, Germany) in rapid scanning mode, operated with a time-resolution of 200 ms at spectral resolution of 2 cm^{-1} unless noted otherwise. Time-resolved recording of the absorbance spectra was conducted before, during, and after illumination. Time-dependent sets of difference spectra were calculated by subtraction of a reference, obtained by averaging the spectra before start of the illumination protocol, from the whole set. Each set of difference spectra was corrected for slight temperature drifts (± 0.1 °C) occurring during the measurement and normalized using bands in the ethylenic region and/or fingerprint region. The data sets were analyzed by singular value decomposition in combination with a rotation procedure as described previously (16).

A Cary 50 spectrophotometer (Varian, Inc.) was used for acquisition of the UV-visible data. Samples were prepared in the same way as described for infrared measurements, but the pellet obtained by centrifugation was placed in a temperature-controlled 50-μm optical path length transmission cuvette consisting of two 10-mm diameter BaF_2 windows and a polytetrafluoroethylene spacer.

RESULTS

Monitoring Dark State Regeneration of C128T by FTIR and UV-visible Difference Spectroscopy—Recombinant channelrhodopsin mutant ChR-C128T used for this study was purified from COS cells and reconstituted in lipid vesicles under dim red light (> 680 nm). In the following, the state of these samples that had never been exposed to light of the visible range will be termed initial dark state (IDA).

Molecular alterations induced by exposure to blue light (470 nm) for 5 min were followed by time-resolved infrared difference spectroscopy. The most significant absorption change occurred at 1661 cm^{-1} and was used as a marker band to monitor changes of the protein. Within 300 ms after the onset of the illumination, the intensity of this negative band was already at its maximum. Together with a positive band at 1646 cm^{-1}, it denotes formation of the P520 intermediate as shown in Fig. 1*A* (illuminated state, conversion 0) and observed in earlier studies (8). Because in flash experiments, both the rise and decay of P520 closely matches the kinetics of the photocurrents measured in *Xenopus* oocytes and HEK cells, P520 intermediates are considered as conducting states and of exceptional interest (2–4). The complete FTIR difference spectrum (illuminated state minus IDA), shown in *blue* in Fig. 1*B*, is predominantly a fingerprint of the transition from the dark state to P520. Two minutes of blue illumination led to the formation of the photostationary state, characterized by a lower but constant intensity of the band at 1661 cm^{-1} (conversion 1 in Fig. 1*A*). The corresponding photostationary state minus IDA difference spectrum is shown in Fig. 1*B* (*red line*). It is an overlay of the P520 spectrum, late photocycle intermediates, and intermediates of the side pathway. The latter is indicated by the reduced bands at 1661 and 1651 cm^{-1} and the typical alterations of the pattern ~1550 cm^{-1} (8).

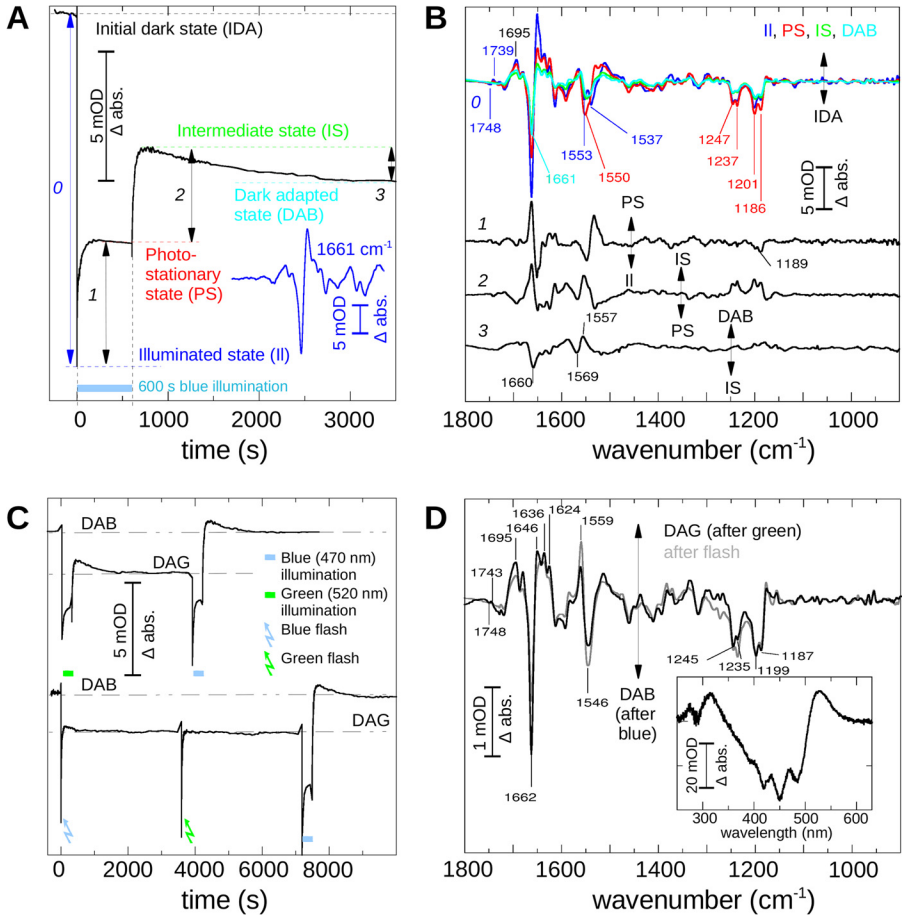

FIGURE 1. **Dark states and photostationary states of C128T channelrhodopsin.** *A*, ChR2 mutant C128T, reconstituted in L-α-phosphatidylcholine vesicles in the dark, was illuminated 600 s by blue (470 nm) light. The spectral changes of optical density (*OD*) of the prominent 1661 cm^{-1} band (as shown in the *inset*, *blue line*) are drawn as a function of time (*black line*). The illumination period is marked as a *blue bar*. We note the formation of the illuminated state (*blue*) immediately after the start of the illumination. It then evolves into a photostationary state (*red*). After the end of the illumination, the system converts via an intermediate state (*light green*) into a dark-adapted state (DAB, *dark green*). *Underlined numbers* indicate conversions used to calculate double difference spectra as shown in the next panel. *B*, infrared difference spectra photoproduct minus dark state of the illuminated state (measured immediately after start of illumination; *blue*), the photostationary state (*red*), the intermediate state (*light green*), and the dark-adapted state (DAB; *green*), achieved after 3600 s in the dark. For better comparison, the spectra were scaled. Double differences of the interconversions between these states were then calculated as indicated in *A* and numbered accordingly. *C*, *upper trace*: the same sample as shown in *A* was, after a regeneration period of 3 h after the blue illumination, exposed to a green illumination (300 s; 520 nm), and the intensity at 1661 cm^{-1} was recorded as a function of time. After lights off, the sample evolved into a new dark-adapted state (DAG). A subsequently applied blue illumination of the sample initiated its return into DAG. *Lower trace*: flash illumination, either green or blue, caused the same effect as long green illumination, thereby finally leading to the DAG state (*blue* and *green arrows*). Extended blue illumination (*blue bar*) led back to DAB. *D*, FTIR and UV-visible (*inset*) difference spectrum (double difference) of DAB minus DAG (*black line*). We note differences in the structurally sensitive parts of the spectrum >1600 cm^{-1} as well as in the region indicative for chromophore geometry (1150–1250 cm^{-1}). The double difference between the state induced by flash illumination and DAB is also given for comparison (*gray line*). *abs.*, absorbance.

During the dark period that follows blue illumination, the sample evolves within 1 h via an intermediate state (conversion 2, Fig. 1*A*, and *light green line* in Fig. 1*B*) to a stable dark-adapted state (conversion 3, Fig. 1*A*), which will be termed dark-adapted state after blue (DAB) in the following. The *green* and *cyan* spectra in Fig. 1*B* denote the difference spectra of these two transitions, *i.e.* intermediate state minus IDA and DAB minus IDA, respectively. Interestingly, in the intermediate state 3 min after light the negative band at 1661 cm^{-1} is minimally developed and increases again during formation of DAB. The corresponding FTIR difference spectra shown in Fig. 1*B* reveal that besides 1661 cm^{-1}, bands at 1553, 1247, 1237, 1201, and 1186 cm^{-1} which are all present in the IDA to P520 transition, also remain at a residual level in DAB. For better illustration of the changes that occur during the conversion from one state to the next, the double difference spectra between the illuminated state and the photostationary state (*line 1*), between the photostationary state and the intermediate state (*line 2*), and between the intermediate state and DAB (*line 3*) are additionally given in Fig. 1*B*.

The double difference of the transition (*line 1*) displays bands in the amide I region at 1661 cm^{-1} and in the amide II region ~1550 cm^{-1}, which were previously assigned to the formation of the photocycle side products (8). Only small bands are observed in the region indicative for chromophore geometry (1150–1300 cm^{-1}). Thus, we assume only slight changes of the chromophore geometry during photostationary state formation starting from P520. In contrast, during the transition from the photostationary state to the intermediate state (*line 2*) the chromophore bands are significantly more intense and largely a mirror image of the activating band pattern seen in conversion *0*. Finally, during formation of DAB (*line 3*), shallow bands in

the region of the chromophore C-C stretching modes indicate that the chromophore geometry changes only marginally. Bands in the amide I and amide II region ~1660 cm^{-1} and 1557 cm^{-1} argue for changes of the peptide backbone, and in the case of amide II, suggest changes of the retinal and/or the retinal Schiff base.

Next, we investigated how the dark adapted state formation depends on color and duration of the actinic light. In Fig. 1*C*, the kinetics of the band at 1661 cm^{-1} is shown again, but the illumination of DAB was now performed with green light (520 nm; *upper trace*, *green bar*) instead of blue light.

We observe formation of an illuminated state with a primary contribution of P520, as indicated by the intense 1661 cm^{-1} band in the corresponding FTIR difference spectrum. Similarly to blue illumination, it subsequently evolved into a photostationary state. After the termination of green light, we likewise observed a transient intermediate state. Finally, a new stable dark-adapted state was formed that clearly differed from DAB as indicated by the residual level of the band at 1661 cm^{-1}. In the following, this state will be termed dark-adapted state after green illumination (DAG).

Subsequent blue illumination of DAG (Fig. 1*C*, *upper trace*, *blue* bar) eventually resulted in a return of the sample to DAB as concluded from the final amplitude of the band at 1661 cm^{-1}. In a further experiment, instead of continuous illumination, light flashes were applied (Fig. 1*C*, *lower trace*). Surprisingly, green (520 nm) and blue (470 nm) flashes had the same effect on dark-adapted state formation. In both cases, the intensity at 1661 cm^{-1} remained at the level typical for DAG. DAB could only be restored by extended blue illumination. Interestingly, the intermediate state was not as clearly observed when flash illumination was applied.

Structural differences between the dark adapted states are best seen in the FTIR double difference spectra (DAG minus DAB) between these two states as shown in Fig. 1*D* (*black line*). In addition to the significant difference band at 1661 cm^{-1}, intense bands occur also in the amide II/ethylenic region (1546 cm^{-1}/1559 cm^{-1}) and ~1230 cm^{-1}, indicating different chromophore geometries or chromophore-protein interaction in DAB and DAG. The pattern in the latter region closely resembles the one observed in the photostationary state minus dark state difference spectrum. Bands are likewise broadened and often occur in doublets. Interestingly, we also note a pronounced distinctive pattern in the region of carbonyl vibrations comprising a negative band at 1719 cm^{-1} and a positive band at 1695 cm^{-1}, and a very small bilobe at 1748 (−)/1743 cm^{-1} (+). Finally, the UV-visible difference (DAG minus DAB; *inset*, *black*) demonstrates that the fine-structured absorption maximum ~470 nm is slightly less developed in DAG. Notably, the double difference of the intermediate formed after flash minus DAB (shown as *gray* line) shows almost the same spectral pattern as the DAG minus DAB over the whole spectral range.

Retinal Extraction Experiments—The isomerization state of the chromophore before and after illumination was investigated by extraction and subsequent HPLC analysis of the retinoids. Fig. 2*A* shows the HPLC traces of IDA and of the states at various times after a 5-min blue or green illumination. In Fig. 2, *B* and *C*, the contents of the retinal isoforms are plotted as a function of time after illumination.

The first peak was identified as 13-*cis*-retinal, followed by 11-*cis*, 9-*cis*, and all-*trans* retinal. From IDA, we extracted 22% 13-*cis* and 78% all-*trans* retinal, consistent with earlier extraction experiments (8) and raman data (17).

Because retinal extraction of the photostationary state is not possible, the first extraction of an intermediate state was performed 15 s after the blue or green light was shut off. We observed 37% 13-*cis* and 56% all-*trans* retinal after blue light and 47% 13-*cis* and 43% all-*trans* retinal after green light, and small shares of 9-*cis* and 11-*cis* retinal as shown in Fig. 2, *B* and *C*.

Subsequently, the all-*trans* retinal content decreased further to 24% in a thermal process (59% 13-*cis*), observed 180 s after blue illumination. When green light was applied, the change was even more distinctive (24% all-*trans*-retinal and 64% 13-*cis* retinal). Although the minimal content of all-*trans* retinal was observed 180 s after the blue illumination, its fraction increased again to 41% 3600 s after blue illumination and to 33% after green light. During the experiment, the fractions of 11-*cis* and 9-*cis* retinal constantly increased up to 14 and 22% in case of blue illumination and to 14 and 13% after green light. In a control experiment where samples were kept in complete darkness, the ratio between 13-*cis* and all-*trans* retinal did not change and no other *cis* isomers were observed.

The data underline that thermal isomerizations still occurred after blue or green light was shut off as already concluded from the infrared difference spectra. A significant fraction of 13-*cis* retinal that was transiently formed within minutes after end of the illumination was significantly higher after green in comparison with blue light. Whereas the amount 13-*cis* and all-*trans* retinal nearly returned to its initial contribution on a slow time scale, the share of 9- and 11-*cis* was constantly increasing for hours in the dark.

It is worth mentioning that this finding is not specific to the C128T mutant. Similar slow changes were observed for E123T (CheTA) in which the conducting state decays within 5 ms after the illumination (see supplemental Fig. 1) (18). Despite this accelerated cycling of this mutant, the maximal fraction of 13-*cis* retinal, namely 70%, was reached only ~10 min after the end of blue or green illumination. Even after 1 h, we still observed >60% 13-*cis* retinal. Interestingly, the fraction of 9-*cis* and 11-*cis* retinal increased slightly but constantly during the experiment.

Monitoring Light-induced Switching of C128T by FTIR Spectroscopy—During electrical measurements the conductivity of C128T could be switched on and off by alternating blue and green light (6). We performed a similar experiment with blue (470 nm) and green (520 nm) illumination. Time-resolved FTIR difference spectra were recorded during this procedure. The corresponding kinetics showed however a complicated behavior caused by a strong overlap of several processes that occur in parallel. To identify independent components that contribute to the time-dependent spectral data set, we applied a combination of singular value decomposition and a rotation procedure as described (16). This allowed us to separate the contributions of different superimposed processes and to

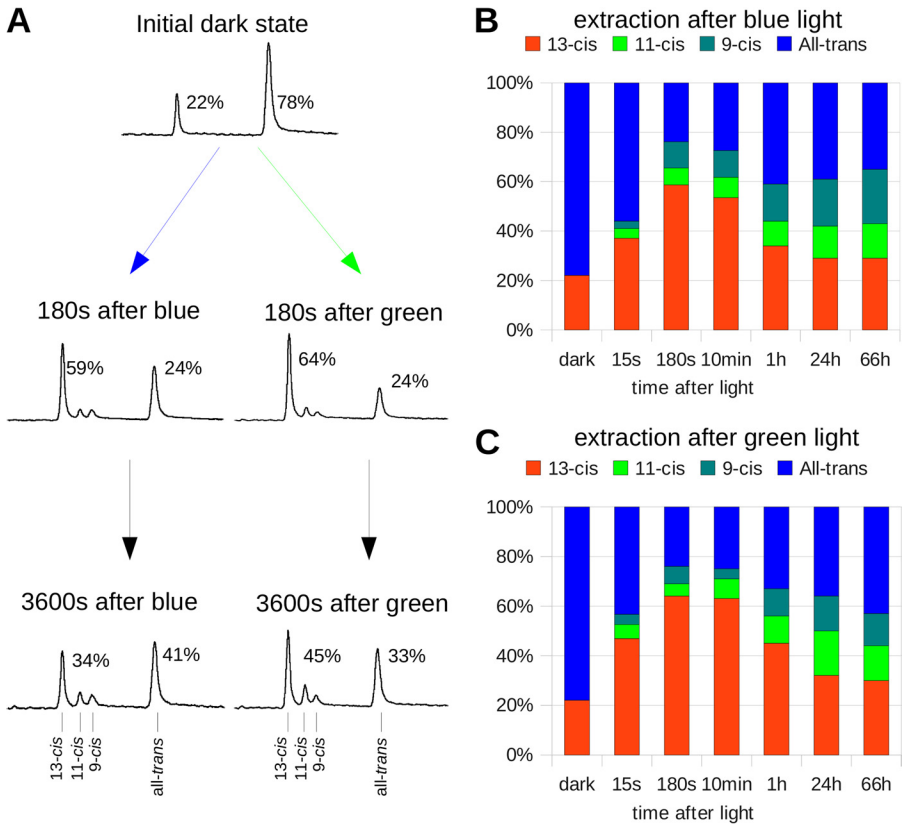

FIGURE 2. **Retinal isomers during the photocycle.** *A*, retinal aldehyde HPLC extraction of different C128T states was performed at the times indicated after a 5-min blue or green illumination. Shown are the data from one single experiment. In the initial dark state, we found a mixture of 22% 13-*cis* and 78% all-*trans*, as reported previously. Surprisingly, after the extended illumination, we found significantly increased contributions of *cis* retinals. The share of 13-*cis* retinal was, however, dependent on illumination conditions; its maximum was reached 180 s after light. We found a slightly lesser maximal amount after a blue illumination (*left column*) than after a green illumination (*right column*). The relaxation into a dark state-like retinal mixture occurred on a very slow timescale that was even slower than the observed spectral alterations. *B*, extracted retinal isomer mixture before and at different times after the illumination; shown are 13-*cis* retinal (*red*), 11-*cis* retinal (*green*), 9-*cis* retinal (*cyan*), and all-*trans* retinal (*blue*). *C*, time course of the extracted retinal isomer mixture after application of a green (520 nm) instead of a blue illumination. *Color* codes are the same as described in *B*.

obtain the pure kinetics and base spectra. By this procedure, four components were identified.

In Fig. 3, the calculated normalized spectral components (*left*) and the corresponding normalized kinetics (*right*) are given. The first component (Fig. 3, *A* and *B*) occurred within seconds ($\tau = 1.7$ s) and remained unchanged during application of the illumination protocol. Interestingly, the bands indicative of changes in the chromophore geometry were broadened and occurred in doublets (1247 and 1237 cm^{-1}; 1202 and 1186 cm^{-1}), similarly to those seen in the photostationary state. Distinct bands seen in the amide I and amide II region may indicate structural changes during its formation.

A second component (Fig. 3, *C* and *D*) was formed in parallel within the first seconds, but it immediately started to decay ($\tau_{on} = 1.6$ s, $\tau_{off} = 66$ s). The second τ value was in accordance with the kinetics of the formation of the photostationary state including formation of side products. The region sensitive to chromophore alterations was characterized by a single band at 1178 cm^{-1}, as known from the P353 intermediate (at 1180 cm^{-1}) of the C128T side reaction.

The third component (Fig. 3, *E* and *F*) arose immediately after light onset. Its formation was not fully resolved, and it disappeared rapidly on a time scale of seconds ($\tau_{on} < 0.3$ s, $\tau_{off} = 2.0$ s). Its dominating spectral feature was the characteristic band at 1661 cm^{-1}, accompanied by small changes in the amide II/ethylenic and chromophore fingerprint region.

The fourth component (Fig. 3, *G* and *H*) was the only one that showed a time-dependent behavior strictly following the alternating blue and green illuminations. The dominating feature was the difference band at 1559/1533 cm^{-1} in the ethylenic region, caused by the Schiff base, which provides a direct correlation to the UV-visible absorption maxima (19), thus identifying a blue- (P480) and a green-absorbing (P520) species. Notably, vibrational changes in the structurally sensitive amide I region at 1661 cm^{-1} and 1625 cm^{-1} were comparatively small in this case. In the fingerprint region characteristic for chromophore C-C stretching vibrations, a distinct pattern including bands at 1237, 1202, 1155, and 1176 cm^{-1} appeared. On the one hand, these patterns showed close similarities with the bands that indicate all-*trans*/13-*cis* isomerization in the spectra of Schiff base protonated bacteriorhodopsin intermediates. However, on the other hand, they were smaller than expected when related to the band intensities in the amide II/ethylenic region. The bilobe at 1748/1741 cm^{-1} indicated involvement of the C=O group of Asp-156 in this conversion (20). Interestingly, similar observations were made when the wild type was illuminated with alternating blue and green light (supplemental Fig. 2).

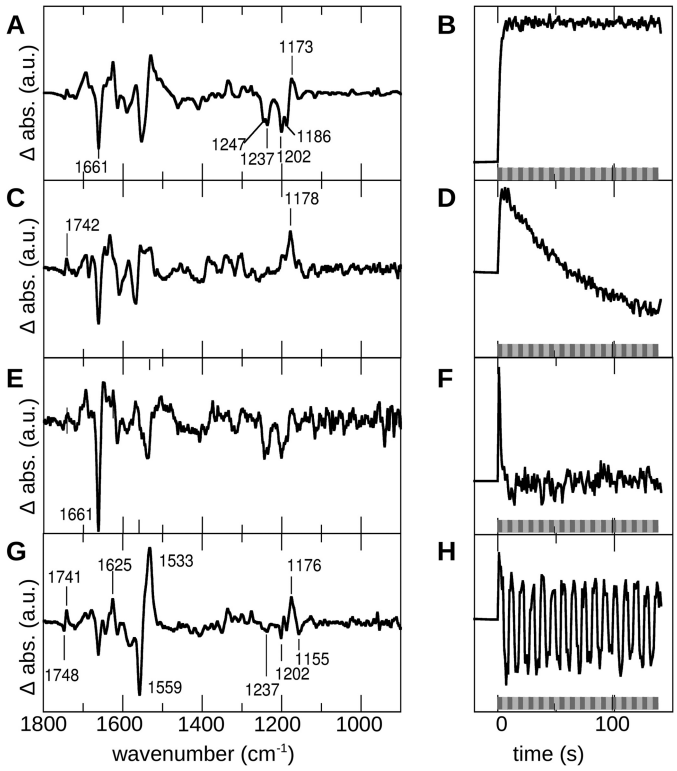

FIGURE 3. **The kinetic data of C128T during alternating green (520 nm) and blue (470 nm) illumination were analyzed by singular value decomposition and rotation procedure.** A dark-adapted sample (DAB) was illuminated with blue (*dark gray bar*) and green (*light gray bar*) light alternatively. Each illumination was performed for 5 s, and then the wavelength of the incident light was immediately changed. Initial spectra were recorded with a time resolution of 200 ms. Subsequent data analysis yielded four main spectral components (b-spectra are scaled; absorbance is given in arbitrary units (*a.u.*); *left column*) that could be separated due to their kinetic behavior (*right column*). The first three components *A–E*, as seen from their kinetics *B–F*, reflect alterations of the protein induced once by the illumination but not directly dependent on the wavelength of incident light. Only the fourth component (*G*) closely followed the illumination procedure (*H*). *abs.*, absorbance.

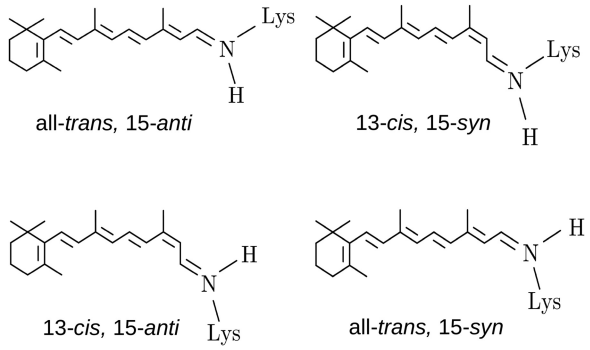

FIGURE 4. **Retinal isomers of retinylidene proteins.** In the bacteriorhodopsin dark-adapted state, either all-*trans*, 15-*anti* or 13-*cis*, 15-*syn* retinal is observed, whereas 13-*cis*, 15-*anti* retinal occurs in the M intermediate structure. In bovine rhodopsin, the switch between all-*trans*, 15-*anti* and all-*trans*, 15-*syn* is capable to switch between the active form and its thermal predecessor.

DISCUSSION

The Dark States of C128T—By FTIR spectroscopy, we showed that samples of the ChR2-C128T mutant that were never exposed to light exist in a unique IDA whose recovery was neither possible by illumination nor by thermal decay. Furthermore, two dark-adapted states were formed after either blue or green light (DAB or DAG, respectively). From the infrared difference spectra, we conclude that the predominant chromophore geometries in these states are different, and consequently, multiple retinal isomerizations must occur in parallel during formation of these states. IDA, DAB, and DAG are each composed of one or more pure intermediates, characterized by a unique, singular protein conformation contributing to different extents to the dark states. The respective spectra of the transitions between IDA and DAB or DAG differ only in their intensities, demonstrating that two dark-adapted intermediates are sufficient to describe the observed spectra and conversions. Similar with earlier electrophysiological work (21, 22), these intermediates are termed D470 and D480. IDA and DAB are both predominantly composed of D480, whereas in DAG, D470 is the main contributing intermediate.

Dark State Formation Depends on the Duration of Incident Light—Interestingly, short light flashes applied to IDA, DAB, or DAG are unable to mediate the shift of dark state composition, and only DAG is formed in either case (compare Fig. 1). DAB must therefore result from a multi-photon process in which a blue or UV-shifted intermediate, most likely P380 of the side pathway, is excited, whereas DAG is formed by thermal decay of P380 (see Fig. 5). From resonance Raman studies, it is known that this pathway includes Schiff base hydrolysis and transient detachment of the retinal from the protein (23). This might account for the formation of a photostationary mixture of several isomers, including 11- and 9-*cis* retinal. However, whereas the distribution between 13-*cis* and all-*trans* was reversible at a long timescale, the share of 9- and 11-*cis* was constantly increasing in a thermal reaction. We therefore assume that these isomers are not directly involved in the photocycle but are rather products of photocycle side reactions. Note that the pathway, involving DAB, is the one that is populated during electrical experiments on neuronal cells or oocytes when a blue illumination of seconds is used as an activating trigger (9).

Retinal Conformational Changes—Interestingly, whereas former HPLC studies with wild type ChR2 in detergent (8, 24) suggested no significant light-induced alterations of retinal isomers, in lipid vesicles, we now observe a considerable transient increase of 13-*cis* retinal at the cost of all-*trans* retinal. The change is significantly higher after green than after blue light. Although the FTIR spectra indicate the existence of conversions between several different retinal isomers, HPLC extraction experiments of DAB and DAG reported predominantly two isomers, namely 13-*cis* and all-*trans* retinal. Accordingly, we conclude that, apart from *trans*/*cis*, also *syn*/*anti* isomerizations of the retinal C=N Schiff base bond also contribute to the retinal fingerprint of the spectra. S*yn*/*anti* isomerizations as described here are not unusual for retinal proteins and were observed for bacteriorhodopsin during thermal dark adaptation, with the dark adapted state consisting of a 1:1 mixture of all-*trans*, 15-*anti*, and 13-*cis*, 15-*syn* retinal (Fig. 4). Upon light adaptation, a single form containing only all-*trans*, 15-*anti* retinal is adopted (25) from which the H^+-transporting photocycle starts by light-induced all-*trans* to 13-*cis* isomerization. In analogy, we suggest that in ChR2-C128T the two isoforms all-

trans, 15-*anti* retinal and 13-*cis*, 15-*syn* retinal stabilize two inactive forms, because in both cases, the Schiff base proton is in a position that enables formation of the salt bridge with the counter ion, as it occurs in bacteriorhodopsin (Fig. 4). Furthermore, from bovine rhodopsin, it is known that isomerization from all-*trans*, 15-*anti* retinal to all-*trans*, 15-*syn* retinal is capable of switching this receptor from an active (metarhodopsin II) to an inactive (metarhodopsin III) form (26). Similarly, in the ChR2-C128T dark states, a *syn*/*anti* isomerization leading to either 13-*cis*, 15-*anti* or all-*trans*, 15-*syn* retinal could trigger the formation of the conducting state as already surmised previously (8).

Interestingly, slow alterations of the retinal conformation are not only seen with slow ChR2-C128T but also with fast ChR2-E123T, in which the conducting state vanishes within milliseconds after light. In this mutant, the maximal fraction of 13-*cis* retinal is extracted 10 min after illumination (compare supplemental Fig. 1). So far, no spectral alterations could be observed for this mutant, which go along with this slow process.

Disentangling the Photocycle Intermediates—By illumination with either blue or green light, the recording of a pure spectrum of any photocycle intermediate is not possible due to overlapping reactions. But in electrical experiments, the conducting and non-conducting states could be switched by alternating blue and green light (6). For spectroscopic investigation of these conversions, we performed comparable FTIR experiments, in which the spectral changes could be separated into four single components. However, only one component showed exactly the same behavior as the electrical measurements and followed the alternating green and blue light (compare Fig. 3). Thus, this individual component was identified as transition between a blue absorbing state assigned to P480 and a green absorbing state P520. The correlation with the electrical measurements, where P520 was identified as the conducting state, provides a connection between spectra and function of the protein. In the region indicative for chromophore geometry, this important conversion shows strong spectral similarities to the transition between dark state and Schiff base-protonated intermediates in bacteriorhodopsin (27, 28). Consequently, we suggest that the transition between the two light-adapted states P520 and P480 in ChR is triggered by 13-*cis*/all-*trans* retinal isomerization.

It was recently shown that light-adapted ChR exhibits two conducting species with different ion selectivities (21). Here, we show the existence of two dark species that are considered as parent states of the two conducting intermediates in line with the two parallel photocycles described in the literature (22, 29). We propose that one starts from all-*trans*, 15-*anti* retinal (D470), and the other from 13-*cis*, 15-*syn* retinal (D480) (Fig. 5).

Blue or green light absorption starts antidromic isomerization in both cycles, causing partial annihilation of the respective fingerprint bands. However, retinal isomerization that in both cases triggers the transition between a blue and a green absorbing species is also indicated by intense bands in the ethylenic region. Comparatively small bands in the amide I region suggest that only small structural changes of the protein go along with the transition between P520 and P480.

All other components given in Fig. 3 reflect structural changes that occur in common to both the formation of the

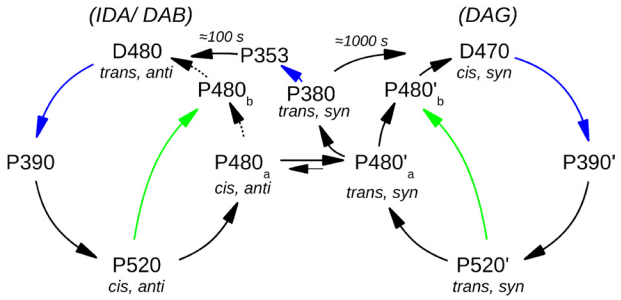

FIGURE 5. **The proposed reaction scheme of ChR2-C128T.** *Black arrows* label thermal reactions, *blue* and *green arrows* label reactions induced by blue (470 nm) and green (520 nm) light, respectively, and *turquoise* arrows label reactions that are triggered by both green and blue light. The proposed isomeric states of the retinal are given in *gray*. The three observed dark states IDA, DAB, and DAG are composed of only two dark species D470 and D480, which occur in different contributions due to the pretreatment of the sample. The unique IDA (from which the reaction starts) is mainly constituted of the species D480, only with minor contributions of D470. Similarly, D480 is the main component of DAB, whereas in DAG, D470 dominates. A photocycle is started by green or blue illumination from either D470 or D480. After the early intermediates (P500 and P500′, accordingly, not shown) and transient SB deprotonation (P390 and P390′), the conducting states P520 and P520′ are formed. The reaction proceeds further to a late intermediate (P480), which is equal or closely similar for both cycles. From this intermediate, D480 and D470 are reformed in a thermal reaction, and the pathway leading to D470 is favored. Alternatively, the side pathway with its intermediate P380 is populated either thermally or light-induced. Although thermal decay of P380 leads only into D470, its excitation by light enables formation of D480 via additional intermediates. Hence, another dark-adapted state (DAB) is only observed after long blue illumination. The D480 species can only be populated in significant amounts through the UV-shifted intermediates of the C128T side pathway (P380, P353, not shown) in a multiphoton reaction.

blue or green absorbing state. The first component describes conformational changes in both states that remain unchanged during the whole illumination period. We suggest that they reflect most probably the adjustment of amino acid residues that later facilitate formation of the conducting pore. We tentatively assign the second component (Fig. 3, *C* and *D*) to increased contributions of side pathway intermediates, and the third component to transiently formed early P390 intermediate, vanishing with the formation of the photostationary state.

A New Reaction Scheme for C128T—Based on our new data and on available electrical measurements, we propose a reaction scheme of ChR2-C128T as shown in Fig. 5, which extends the previously described photocycle (8) and links spectroscopic and electrical measurements. All apparent dark states IDA, DAB, and DAG and transitions between them are compositions of two non-conducting dark isoforms D470 and D480 that dominate the dark states depending on the illumination history.

Because different retinal isomer mixtures must be present in the dark states and thus also in the intermediates, we propose all-*trans*, 15-*anti* retinal in D480 and 13-*cis*, 15-*syn* retinal in D470, in analogy to bacteriorhodopsin. In both cases, light induces retinal isomerization (most probably *trans*/*cis* in the case of D480 and *cis*/*trans* in the case of D470) which starts a reaction cascade that proceeds via P390 and P390′ and leads into conducting P520 and P520′. Thermal decay of the conducting states then leads to the late equilibrium between P480a and P480a′, which constitutes the link between the two cycles. It is also the branching point into the side pathway of UV-shifted P380 and P353. Only light excitation of one or both of these intermediates, most probably P380, opens the pathway

back to D480. This further explains why blue flashes fail to restore DAB but lead, similar to green light, to DAG, mainly constituted of D470. Starting from P480, both dark states can be formed in a thermal pathway, but formation of D470 must strongly be favored as major contributions of D480 are not observed after flash. Due to the light sensitivity of both of the P520 intermediates, green illumination can shortcut the photocycle (*green arrows*).

Outlook—In this study, we have shown by a combination of UV-visible and vibrational spectroscopy and HPLC analysis that the two dark states of ChR2-C128T are structurally different and that color and duration of the actinic illumination are major determinants for the dark equilibria between D470 and D480 as well as for the extent of side product formation (P380 and P353). These findings certainly have profound consequences for the stationary contribution of the two open states, the degree of inactivation, and the ion composition of the photocurrent whenever ChRs are employed in optogenetic experiments under high light conditions or rapid flash stimulation (30).

Acknowledgments—We acknowledge Brian Bauer, Anja Koch, and Roman Kazmin for technical support in sample preparation and Martha Sommer for critical reading of the manuscript.

REFERENCES

1. Kato, H. E., Zhang, F., Yizhar, O., Ramakrishnan, C., Nishizawa, T., Hirata, K., Ito, J., Aita, Y., Tsukazaki, T., Hayashi, S., Hegemann, P., Maturana, A. D., Ishitani, R., Deisseroth, K., and Nureki, O. (2012) Crystal structure of the channelrhodopsin light-gated cation channel. *Nature* **482,** 369–374
2. Bamann, C., Kirsch, T., Nagel, G., and Bamberg, E. (2008) Spectral characteristics of the photocycle of channelrhodopsin-2 and its implication for channel function. *J. Mol. Biol.* **375,** 686–694
3. Ernst, O. P., Sánchez Murcia, P. A., Daldrop, P., Tsunoda, S. P., Kateriya, S., and Hegemann, P. (2008) Photoactivation of channelrhodopsin. *J. Biol. Chem.* **283,** 1637–1643
4. Ritter, E., Stehfest, K., Berndt, A., Hegemann, P., and Bartl, F. J. (2008) Monitoring light-induced structural changes of Channelrhodopsin-2 by UV-visible and Fourier transform infrared spectroscopy. *J. Biol. Chem.* **283,** 35033–35041
5. Nagel, G., Szellas, T., Huhn, W., Kateriya, S., Adeishvili, N., Berthold, P., Ollig, D., Hegemann, P., and Bamberg, E. (2003) Channelrhodopsin-2, a directly light-gated cation-selective membrane channel. *Proc. Natl. Acad. Sci. U.S.A.* **100,** 13940–13945
6. Berndt, A., Yizhar, O., Gunaydin, L. A., Hegemann, P., and Deisseroth, K. (2009) Bi-stable neural state switches. *Nat. Neurosci.* **12,** 229–234
7. Zhang, Y. P., and Oertner, T. G. (2007) Optical induction of synaptic plasticity using a light-sensitive channel. *Nat Methods* **4,** 139–141
8. Stehfest, K., Ritter, E., Berndt, A., Bartl, F., and Hegemann, P. (2010) The branched photocycle of the slow-cycling channelrhodopsin-2 mutant C128T. *J. Mol. Biol.* **398,** 690–702
9. Schoenenberger, P., Schärer, Y. P., and Oertner, T. G. (2011) Channelrhodopsin as a tool to investigate synaptic transmission and plasticity. *Exp. Physiol.* **96,** 34–39
10. Stehfest, K., and Hegemann, P. (2010) Evolution of the channelrhodopsin photocycle model. *Chemphyschem* **11,** 1120–1126
11. Molday, R. S., and MacKenzie, D. (1983) Monoclonal-antibodies to rhodopsin: Characterization, cross-reactivity, and application as strutural probes. *Biochemistry* **22,** 653–660
12. Ernst, O. P., Meyer, C. K., Marin, E. P., Henklein, P., Fu, W. Y., Sakmar, T. P., and Hofmann, K. P. (2000) Mutation of the fourth cytoplasmic loop of rhodopsin affects binding of transducin and peptides derived from the carboxyl-terminal sequences of transducin α and γ subunits. *J. Biol. Chem.* **275,** 1937–1943
13. Elgeti, M., Kazmin, R., Heck, M., Morizumi, T., Ritter, E., Scheerer, P., Ernst, O. P., Siebert, F., Hofmann, K. P., and Bartl, F. J. (2011) Conserved Tyr223(5.58) plays different roles in the activation and G-protein interaction of rhodopsin. *J. Am. Chem. Soc.* **133,** 7159–7165
14. Scherrer, P., Mathew, M. K., Sperling, W., and Stoeckenius, W. (1989) Retinal isomer ratio in dark-adapted purple membrane and bacteriorhodopsin monomers. *Biochemistry* **28,** 829–834
15. Bartl, F., Ritter, E., and Hofmann, K. P. (2000) FTIR spectroscopy of complexes formed between metarhodopsin II and C-terminal peptides from the G-protein α- and γ-subunits. *FEBS Lett.* **473,** 259–264
16. Elgeti, M., Ritter, E., and Bartl, F. J. (2008) New Insights into Light-Induced Deactivation of Active Rhodopsin by SVD and Global Analysis of Time-Resolved UV/Vis- and FTIR-Data. *Zeitschrift für Physikalische Chemie* **222,** 1117–1129
17. Radu, I., Bamann, C., Nack, M., Nagel, G., Bamberg, E., and Heberle, J. (2009) Conformational changes of channelrhodopsin-2. *J. Am. Chem. Soc.* **131,** 7313–7319
18. Gunaydin, L. A, Yizhar, O., Berndt, A., Sohal, V. S., Deisseroth, K., and Hegemann, P. (2010) Ultrafast optogenetic control. *Nat. Neurosci.* **13,** 387–392
19. Aton, B., Doukas, A. G., Callender, R. H., Becher, B., and Ebrey, T. G. (1977) Resonance Raman studies of the purple membrane. *Biochemistry* **16,** 2995–2999
20. Nack, M., Radu, I., Gossing, M., Bamann, C., Bamberg, E., von Mollard, G. F., and Heberle, J. (2010) The DC gate in Channelrhodopsin-2: crucial hydrogen bonding interaction between C128 and D156. *Photochem. Photobiol. Sci.* **9,** 194–198
21. Berndt, A., Prigge, M., Gradmann, D., and Hegemann, P. (2010) Two open states with progressive proton selectivities in the branched channelrhodopsin-2 photocycle. *Biophys. J.* **98,** 753–761
22. Hegemann, P., Ehlenbeck, S., and Gradmann, D. (2005) Multiple photocycles of channelrhodopsin. *Biophys. J.* **89,** 3911–3918
23. Bruun, S., Naumann, H., Kuhlmann, U., Schulz, C., Stehfest, K., Hegemann, P., and Hildebrandt, P. (2011) The chromophore structure of the long-lived intermediate of the C128T channelrhodopsin-2 variant. *FEBS Lett.* **585,** 3998–4001
24. Nack, M., Radu, I., Bamann, C., Bamberg, E., and Heberle, J. (2009) The retinal structure of channelrhodopsin-2 assessed by resonance Raman spectroscopy. *FEBS Lett.* **583,** 3676–3680
25. Patzelt, H., Simon, B., terLaak, A., Kessler, B., Kühne, R., Schmieder, P., Oesterhelt, D., and Oschkinat, H. (2002) The structures of the active center in dark-adapted bacteriorhodopsin by solution-state NMR spectroscopy. *Proc. Natl. Acad. Sci. U.S.A.* **99,** 9765–9770
26. Bartl, F. J., Ritter, E., and Hofmann, K. P. (2001) Signaling states of rhodopsin: absorption of light in active metarhodopsin II generates an all-trans-retinal bound inactive state. *J. Biol. Chem.* **276,** 30161–30166
27. Marcus, M. A., and Lewis, A. (1978) Resonance Raman spectroscopy of the retinylidene chromophore in bacteriorhodopsin (bR570), bR560, M421, and other intermediates: structural conclusions based on kinetics, analogues, models, and isotopically labeled membranes. *Biochemistry* **17,** 4722–4735
28. Marrero, H., and Rothschild, K. J. (1987) Conformational changes in bacteriorhodopsin studied by infrared attenuated total reflection. *Biophys. J.* **52,** 629–635
29. Nikolic, K., Grossman, N., Grubb, M. S., Burrone, J., Toumazou, C., and Degenaar, P. (2009) Photocycles of channelrhodopsin-2. *Photochem. Photobiol.* **85,** 400–411
30. Yizhar, O., Fenno, L. E., Davidson, T. J., Mogri, M., and Deisseroth, K. (2011) Optogenetics in neural systems. *Neuron* **71,** 9–34